ACS APPLIED MATERIALS & INTERFACES

Research Article

Cite This: ACS Appl. Mater. Interfaces 2017, 9, 40471-40476

www.acsami.org

Influence of High-Energy Proton Irradiation on β-Ga_2O_3 Nanobelt Field-Effect Transistors

Gwangseok Yang,[†] Soohwan Jang,[‡] Fan Ren,[§] Stephen J. Pearton,[∥] and Jihyun Kim*[,†]

[†]Department of Chemical and Biological Engineering, Korea University, Seoul 02841, South Korea

[‡]Department of Chemical Engineering, Dankook University, Yongin 16890, South Korea

[§]Department of Chemical Engineering and [∥]Department of Materials Science and Engineering, University of Florida, Gainesville, Florida 32611, United States

Supporting Information

ABSTRACT: The robust radiation resistance of wide-band gap materials is advantageous for space applications, where the high-energy particle irradiation deteriorates the performance of electronic devices. We report on the effects of proton irradiation of β-Ga_2O_3 nanobelts, whose energy band gap is ~4.85 eV at room temperature. Back-gated field-effect transistor (FET) based on exfoliated quasi-two-dimensional β-Ga_2O_3 nanobelts were exposed to a 10 MeV proton beam. The proton-dose- and time-dependent characteristics of the radiation-damaged FETs were systematically analyzed. A 73% decrease in the field-effect mobility and a positive shift of the threshold voltage were observed after proton irradiation at a fluence of 2×10^{15} cm^{-2}. Greater radiation-induced degradation occurs in the conductive channel of the β-Ga_2O_3 nanobelt than at the contact between the metal and β-Ga_2O_3. The on/off ratio of the exfoliated β-Ga_2O_3 FETs was maintained even after proton doses up to 2×10^{15} cm^{-2}. The radiation-induced damage in the β-Ga_2O_3-based FETs was significantly recovered after rapid thermal annealing at 500 °C. The outstanding radiation durability of β-Ga_2O_3 renders it a promising building block for space applications.

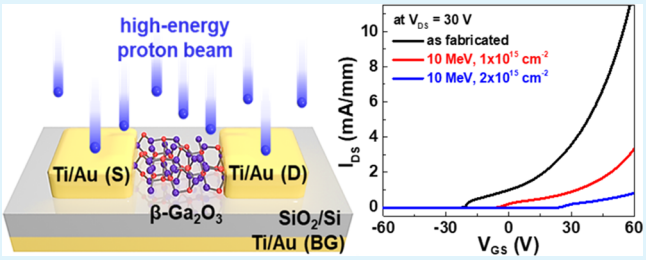

KEYWORDS: *gallium oxide, wide-band gap semiconductors, proton irradiation, two-dimensional materials, thermal annealing*

INTRODUCTION

Radiation hardness of semiconductor devices is indispensable for space missions because these devices are continuously exposed to fluxes of various energetic particles, including high-energy protons, electrons, neutrons, and heavy ions in space.[1,2] The electronics in spacecraft performing tasks in earth's orbit must consider three major sources of radiation: (i) galactic cosmic rays, (ii) energetic particles trapped in the van Allen belts, and (iii) solar particle events (SPEs). Among these, SPEs contain high-energy protons (>10 MeV) at a typical fluence of 10^{10} cm^{-2}, and the occurrence of 1−2 SPEs every solar cycle is predicted.[3,4] Because protons constitute the primary component of the three major radiation sources, we investigated the influence of high-energy proton irradiation on β-Ga_2O_3, which is an ultrawide-band gap semiconductor material.

Wide-band gap semiconductors are typically applicable in radiation-robust devices because of their high bond strengths.[5−9] The unique properties of wide-band gap materials, including their high-temperature capability and strong atomic bonding energy, enable them to operate under harsh conditions.[10−13] β-Ga_2O_3, an emerging semiconductor material, has attracted great attention due to its extraordinary characteristics, such as an ultrawide energy band gap of ~4.85 eV, a large breakdown electric field of ~8 MV/cm, and a high saturation electron velocity of 2×10^7 cm/s.[14,15] These desirable properties have allowed the application of β-Ga_2O_3 in solar-blind photodetectors, high-breakdown Schottky diodes, and high-power field-effect transistors (FETs).[16−18]

Furthermore, β-Ga_2O_3 is currently receiving tremendous attention in the field of nanoelectronics because it can be mechanically cleaved from a freestanding substrate, although it is not a van der Waals material. Back-gated FETs, depletion/enhancement mode FETs, solar-blind photodetectors, and high-temperature FETs have been fabricated using mechanically exfoliated β-Ga_2O_3.[19−22] However, radiation effects on nanoscale β-Ga_2O_3 have not been investigated despite its higher formation energy of vacancy defect (for Ga vacancy in β-Ga_2O_3, it is 53.3 eV) compared to that of other wide-band gap materials (7.02 eV for GaN (Ga vacancy) and 3.3 eV for 3C-SiC (Si vacancy)).[23−25] Only few studies have been reported on the radiation tolerance of bulk and thin-film β-Ga_2O_3. The effects of 1.5 MeV electron irradiation on bulk β-Ga_2O_3 vertical rectifiers and 5 MeV proton irradiation damage on β-Ga_2O_3-based photodetectors have been reported.[26,27] These β-Ga_2O_3-

Received: September 12, 2017
Accepted: October 30, 2017
Published: October 30, 2017

DOI: 10.1021/acsami.7b13881
ACS Appl. Mater. Interfaces 2017, 9, 40471−40476

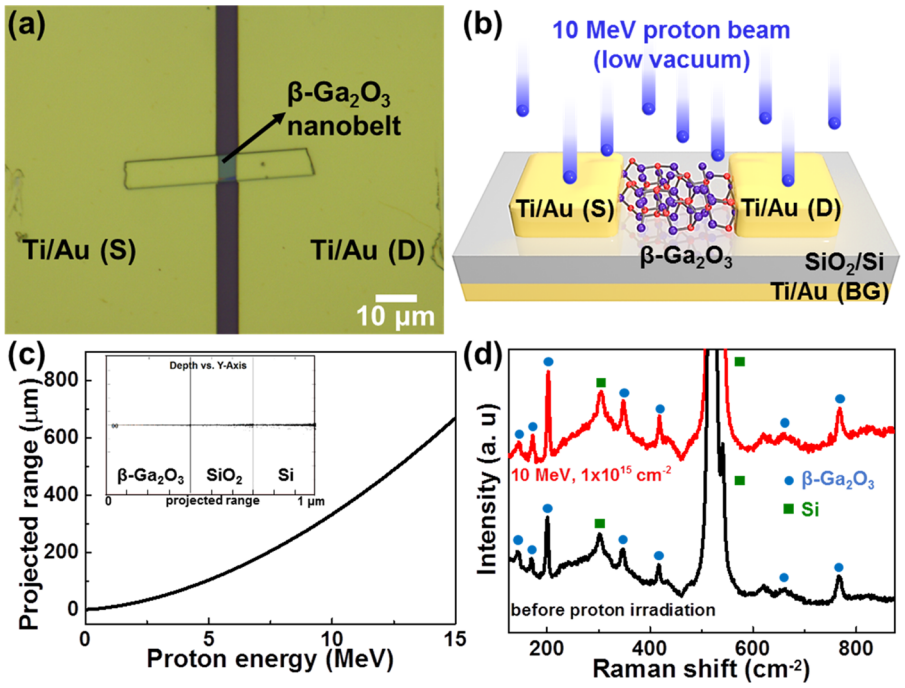

Figure 1. (a) Optical microscopy image of a β-Ga_2O_3 nanobelt FET, (b) schematic of the proton irradiation on a β-Ga_2O_3 nanobelt FET, (c) projected range of the proton on bulk β-Ga_2O_3 estimated by Stopping and Range of Ions in Matter (SRIM) simulation (inset shows the penetration depth profile of 10 MeV protons on β-Ga_2O_3/SiO_2/Si (thickness of 400/300/300 nm)), (d) Raman spectra of the β-Ga_2O_3 nanobelt before and after proton irradiation (10 MeV, 1×10^{15} cm^{-2}).

based devices display robust radiation hardness, which is comparable to that of GaN. In this article, we report on the effects of 10 MeV proton irradiation at various doses and subsequent thermal annealing on β-Ga_2O_3 nanobelt-based FETs. The electrical and structural properties of these quasi-two-dimensional (2D) β-Ga_2O_3 nanobelts were analyzed before and after proton irradiation and subsequent thermal annealing.

EXPERIMENTAL DETAILS

Fabrication of β-Ga_2O_3 Nanobelt FETs. Quasi-2D β-Ga_2O_3 nanobelts were separated from an unintentionally n-doped single crystalline β-Ga_2O_3 substrate (Tamura Corporation) by a mechanical exfoliation method, where the facile cleavage planes are (100) and (001). The nanobelts were transferred onto a SiO_2/p^{++} Si (300 nm/525 μm) substrate; a back-gate electrode (Ti/Au (20/80 nm)) was predeposited on the backside of the substrate using an electron-beam evaporator. Source and drain electrodes (Ti/Au (50/100 nm)) were defined by standard photolithography. The optical microscopy image of the fabricated β-Ga_2O_3 nanobelt-based FET is shown in Figure 1a.

Characterization. The thickness of the quasi-2D β-Ga_2O_3 nanobelt was measured by atomic force microscopy (Innova, Bruker). The effects of proton irradiation on the electrical and optical properties of the β-Ga_2O_3 nanobelt were investigated using a semiconductor parameter analyzer (4155C, Agilent) connected to a probe station and micro-Raman spectrometry with a diode-pumped solid-state 532 nm laser (Omicron-Laserage) under back-scattering geometry, respectively. Rapid thermal annealing (RTA, MILA-3000, ULVAC-RIKO) was performed at 400 and 500 °C for 30 s under N_2 atmosphere to eliminate the damage induced by the proton irradiation.

Proton Irradiation. Figure 1b shows a schematic of the quasi-2D β-Ga_2O_3 nanobelt-based FET, which was subjected to high-energy proton fluxes. The 10 MeV proton beam was generated using the MC-50 Cyclotron at the Korea Institute of Radiological and Medical Science. The proton beam was injected into a low-vacuum chamber, in which the β-Ga_2O_3-based devices were loaded, facing the proton beam. The average beam current, measured by a Faraday cup, was 100 nA during the proton irradiation process. Proton fluence, which were controlled by the duration of proton irradiation, were up to 2×10^{15} cm^{-2}. The duration of proton irradiation was 1018 and 2036 s, which corresponds to the fluence of 1×10^{15} and 2×10^{15} cm^{-2}, respectively. The proton beam uniformity was characterized by using a radiation sensitive film (Gafchromic MD-V2). The proton beam was uniformly emitted from MC-50 Cyclotron over an area of 1 cm × 1 cm. The electrical and optical characterizations were performed 3 days after the proton irradiation because of safety regulations. The projected range of the 10 MeV proton beam was calculated using the Stopping and Range of Ions in Matter (SRIM) program.[28]

RESULTS AND DISCUSSION

Figure 1c shows the projected range of the proton beam, estimated from the SRIM program. The penetration depth of the 10 MeV proton beam for β-Ga_2O_3 is approximately 332 μm, which exceeds the thickness of the exfoliated β-Ga_2O_3 flake (~400 nm). Therefore, most of the protons pass through the β-Ga_2O_3/SiO_2 (thickness of 400/300 nm) structure, as shown in the inset of Figure 1c. These simulation results indicate that the defects induced by the 10 MeV proton beam should be uniformly distributed throughout the β-Ga_2O_3 flake. The proton-induced damage was also evaluated by micro-Raman spectroscopy, before and after 10 MeV proton irradiation. The Raman spectra of the β-Ga_2O_3 flakes show several Raman active modes, which correspond to ~142 (B_g), ~169 (A_g), ~201 (A_g), ~348 (A_g), ~416 (A_g), ~662 (A_g), and ~767 (A_g) cm^{-1}, as shown in Figure 1d.[29] No noticeable change in these modes was observed after proton irradiation, which indicates that defects generated by the proton flux did not produce any strain-induced Raman shift.

Proton-dose-dependent output (drain−source current vs drain−source voltage, I_{DS}−V_{DS}) and transfer characteristics (drain−source current vs gate−source voltage, I_{DS}−V_{GS}) of the quasi-2D β-Ga_2O_3 nanobelt FET with back-gate configuration are shown in Figures 2 and S1. Its output characteristics with

DOI: 10.1021/acsami.7b13881
ACS Appl. Mater. Interfaces 2017, 9, 40471−40476

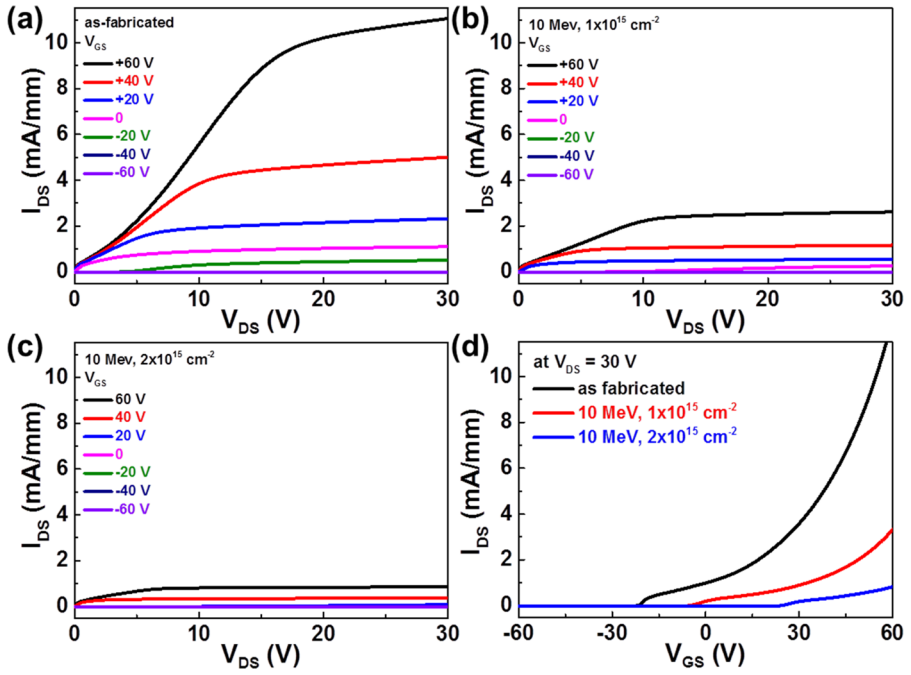

Figure 2. Output characteristics (I_{DS}–V_{DS}) of the β-Ga_2O_3 nanobelt FET before and after 10 MeV proton irradiation at different doses: (a) as fabricated, (b) 1×10^{15} cm^{-2}, and (c) 2×10^{15} cm^{-2}. (d) Transfer characteristics (I_{DS}–V_{GS}) of the β-Ga_2O_3 nanobelt FET at V_{DS} = +30 V before and after 10 MeV proton irradiation at different doses.

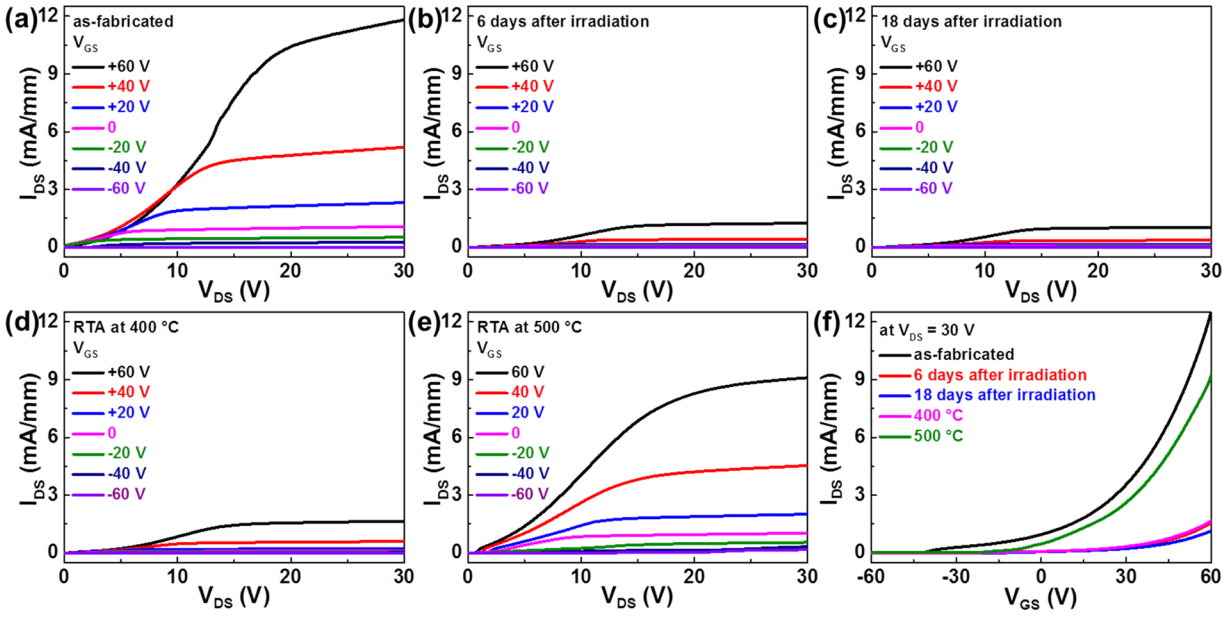

Figure 3. Output characteristics of β-Ga_2O_3 nanobelt FET with time and temperature of RTA after 10 MeV proton irradiation at a fluence of 1×10^{15} cm^{-2}: (a) as fabricated, (b) 6 days after proton irradiation, (c) 18 days after proton irradiation, (d) after RTA at 400 °C, and (e) after RTA at 500 °C. (f) Time and temperature dependent transfer characteristics of β-Ga_2O_3 nanobelt FET at V_{DS} = +30 V.

time and temperature of RTA after 10 MeV proton irradiation at a fluence of 1×10^{15} cm^{-2} are represented in Figure 3. A typical n-type behavior, with a decrease in I_{DS} with decreasing V_{GS}, was observed in the as-fabricated devices. In general, unintentionally doped β-Ga_2O_3 shows n-type conductivity owing to its oxygen vacancies and unintentional impurities.[30,31] The conductivity of the β-Ga_2O_3 flakes decreased with increasing the proton dose to 2×10^{15} cm^{-2}. The removal of the free carriers due to the introduction of radiation-induced deep traps leads to the deterioration of the electrical conductivity,[1,2,32] as reported previously for samples irradiated with both electrons and protons.[26,27] Another electrical parameter influenced by the proton irradiation is the field-effect electron mobility (μ_{fe}). μ_{fe} of β-Ga_2O_3 nanobelt FET was estimated by the following equation, $\mu_{fe} = (g_m \cdot L)/(W \cdot C \cdot V_{DS})$, where g_m, L, W, and C are the transconductance, channel length, channel width, and oxide capacitance, respectively. The μ_{fe} value decreased from 2.9 to 0.78 cm^2/V s with an increasing the proton dose to 2×10^{15} cm^{-2}. The normalized μ_{fe} as a function of proton doses is shown in Figure 4a. μ_{fe} was reduced

DOI: 10.1021/acsami.7b13881
ACS Appl. Mater. Interfaces 2017, 9, 40471–40476

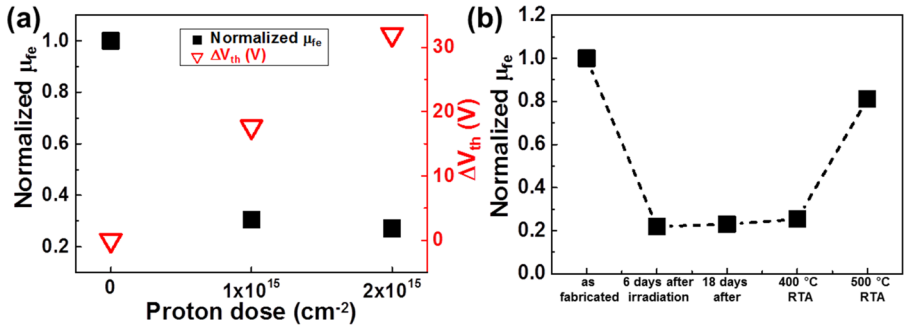

Figure 4. (a) Normalized μ_{fe} and ΔV_{th} as a function of proton doses, (b) RTA-dependent normalized μ_{fe} with respect to time and temperature.

by 73% after proton irradiation at a fluence of 2×10^{15} cm^{-2}. The decrease of μ_{fe} can be explained by increased Coulombic scattering by the radiation-induced defects.[2,5] A positive shift in the threshold voltage (ΔV_{th}) and reduction of I_{DS} were observed in the I_{DS}–V_{GS} curve, as shown in Figures 2d and S1. ΔV_{th} increased with increasing proton dose, which can be explained by the removal of electrons by trapping and introduction of acceptor-type radiation-induced states. The ΔV_{th} can be estimated by the sum of the V_{th} shift caused by the oxide trap (V_{ot}) and interfacial trap (V_{it}), which can be expressed as $\Delta V_{th} = \Delta V_{ot} + \Delta V_{it}$. For n-channel transistors, an increase in the interfacial trap density results in a positive shift in V_{th}, whereas an increase in the oxide trap density typically leads to a negative shift in V_{th}.[33−35] Because the proton-irradiated quasi-2D β-Ga_2O_3 nanobelt FETs showed a positive shift in the V_{th}, the effect of the interfacial traps seems dominant compared to that of the oxide traps. Although proton irradiation induced a large change in μ_{fe}, V_{th}, and the drain–source on-resistance (R_{DS}(on)) values (measured in the linear region before knee voltage), only a nominal change in the on/off ratio was observed, as shown in Figure S1. Proton-dose-dependent electrical parameters, μ_{fe}, normalized μ_{fe}, R_{DS}(on), V_{th}, and the on/off ratio, are summarized in Table 1. The

Table 1. Summary of the Electrical Parameters of the β-Ga_2O_3 Nanobelt FET before and after 10 MeV Proton Irradiation at Different Doses

	as fabricated	10 MeV, 1×10^{15} cm^{-2}	10 MeV, 2×10^{15} cm^{-2}
field-effect mobility (μ_{fe}, cm^2/V s)	2.9	0.88	0.78
normalized μ_{fe}	1	0.31	0.27
R_{DS} (on) (kΩ mm)	1.4	4.8	11
V_{th} (V)	−8.2	9.4	23.7
on/off ratio	7.0×10^7	2.3×10^7	7.5×10^7

degradation of the β-Ga_2O_3 nanobelt FETs caused by proton irradiation is comparable to those of AlGaN/AlN/GaN-based high electron-mobility transistors.[36,37] This indicates the great potential of β-Ga_2O_3 for application in radiation-hard semiconductor devices.

The *Y*-function method was used to evaluate the effects of the high-energy proton irradiation on the channel resistance (R_{ch}) and contact resistance (R_c) of the β-Ga_2O_3 nanobelt FETs. The *Y*-function method is applicable to 2D material-based FETs because it enables an assessment of the transport characteristics of nanoscale materials. The *Y*-function method that was originally developed to analyze a metal-oxide-semiconductor FET allows us to extract the device characteristics from a transfer curve when V_{DS} is much smaller than V_{GS}. The *Y*-function is defined as, $Y = I_{DS}/g_m^{1/2} = (\mu_0 \cdot C_{OX} \cdot W \cdot V_{DS}/L)^{1/2} \cdot (V_{GS} - V_{th})$, where, μ_0 is the low-field mobility.[38,39] Proton-dose-dependent electrical properties extracted by the *Y*-function method are summarized in Table 2. μ_0 decreased by

Table 2. Summary of the Electrical Parameters of the β-Ga_2O_3 Nanobelt FET Extracted by the *Y*-Function Method before and after 10 MeV Proton Irradiation at Different Doses

	as fabricated	10 MeV, 1×10^{15} cm^{-2}	10 MeV, 2×10^{15} cm^{-2}
low-field mobility (μ_0, cm^2/V s)	238	89.7	32.6
normalized μ_0	1	0.38	0.14
R_{ch} (Ω mm)	36.7	132	504
R_c (Ω mm)	606	716	837
R_{ch}/R_{total} (%)	3	8	23

86% after proton irradiation at a fluence of 2×10^{15} cm^{-2}. The μ_0 value, obtained by the *Y*-function method is higher than μ_{fe} because μ_{fe} is generally underestimated owing to R_c. From the calculated μ_0 and V_{th}, R_{ch} can be obtained.[40,41] Because the total resistance (R_{tot}) is composed of R_{ch} and R_c, the contribution of each resistance at different conditions of proton irradiation can be explored. Although both R_c and R_{ch} increased after proton irradiation, a noticeable change in R_{ch} was observed compared to that in R_c. The proportion of R_{ch} in R_{tot} increased from 3 to 23% with increasing proton dose, which indicates that the conductive channel of β-Ga_2O_3 is more susceptible to proton irradiation compared to the contact between the metal and β-Ga_2O_3. Therefore, the main cause of the decline in the electrical performances of the β-Ga_2O_3 nanobelt FETs is inferred to be radiation-induced damage in its conductive channel.

Radiation-induced defects can often be eliminated by recombining with other defects or impurities, even at room temperature.[1,2] We also investigated the thermal removal of the radiation defects. The time-dependent output and transfer characteristics of the quasi-2D β-Ga_2O_3 nanobelt FET are shown in Figures 3 and 4b. The value of μ_{fe} decreased by 78% after 10 MeV proton irradiation at a fluence of 1×10^{15} cm^{-2}. The quasi-2D β-Ga_2O_3-based FET showed no change in the electrical properties when it was measured 18 days after the proton irradiation, indicating no self-recovery at room temperature. Further, RTA was performed to accelerate the restoration of the radiation-induced defects. The electrical characteristics of the quasi-2D β-Ga_2O_3-based FET recovered dramatically with increasing RTA temperatures. The μ_{fe} value reached 81% of its original value after RTA at 500 °C. The β-Ga_2O_3 nanobelt

DOI: 10.1021/acsami.7b13881
ACS Appl. Mater. Interfaces 2017, 9, 40471−40476

FETs did not operate normally at the higher RTA temperature (600 °C) owing to high-temperature-induced degradation.

CONCLUSIONS

High-energy protons were used to produce radiation-induced defects in β-Ga_2O_3 nanobelts obtained by mechanical exfoliation. Optical and electrical characterizations were performed on the fabricated β-Ga_2O_3 nanobelt FETs before and after proton irradiation at an energy of 10 MeV, with a fluence of up to 2×10^{15} cm^{-2}. The μ_{fe} value decreased by 73% after proton irradiation but recovered to 81% of its initial value after RTA at 500 °C. However, the on/off ratio was hardly affected by proton irradiation. The contribution of R_{ch} to R_{total} increased with increasing proton dose, which indicates that the degradation in the conductive channel is greater compared to that in the contact between the metal electrode and β-Ga_2O_3 under proton irradiation. The decline in the electrical performance of the exfoliated β-Ga_2O_3 nanobelt FETs is comparable to the results previously reported for GaN-based devices. The radiation-induced defects were hardly repaired at room temperature, whereas they were almost fully recovered in terms of the electrical performance after thermal annealing at 500 °C. The robust radiation tolerance of the quasi-2D β-Ga_2O_3 nanobelt renders it a potentially useful material for space applications.

ASSOCIATED CONTENT

Supporting Information

The Supporting Information is available free of charge on the ACS Publications website at DOI: 10.1021/acsami.7b13881.

Transfer characteristics of the β-Ga_2O_3 nanobelt FET before and after 10 MeV proton irradiation (PDF)

AUTHOR INFORMATION

Corresponding Author

*E-mail: hyunhyun7@korea.ac.kr.

ORCID

Jihyun Kim: 0000-0002-5634-8394

Notes

The authors declare no competing financial interest.

ACKNOWLEDGMENTS

This research was supported by the Korea Institute of Energy Technology Evaluation and Planning (KETEP), the Ministry of Trade, Industry, and Energy (MOTIE) of Korea (No. 20172010104830), and the Space Core Technology Development Program (2017M1A3A3A02015033) through the National Research Foundation of Korea funded by the Ministry of Science, ICT and Future Planning of Korea. The work at UF was sponsored by the Department of the Defense, Defense Threat Reduction Agency, HDTRA1-17-1-011, monitored by Jacob Calkins.

REFERENCES

(1) Claeys, C.; Simoen, E. *Radiation Effects in Advanced Semiconductor Materials and Devices*; Springer, 2002.

(2) Pearton, S. J.; Deist, R.; Ren, F.; Liu, L.; Polyakov, A. Y.; Kim, J. Review of radiation damage in GaN-based materials and devices. *J. Vac. Sci. Technol., A* **2013**, *31*, No. 050801.

(3) Benton, E. R.; Benton, E. V. Space radiation dosimetry in low-Earth orbit and beyond. *Nucl. Instrum. Methods Phys. Res., Sect. B* **2001**, *184*, 255−294.

(4) Shea, M. A.; Smart, D. F. A summary of major solar proton events. *Sol. Phys.* **1990**, *127*, 297−320.

(5) Pearton, S. J.; Ren, F.; Patrick, E.; Law, M. E.; Polyakov, A. Y. Review—Ionizing Radiation Damage Effects on GaN Devices. *ECS J. Solid State Sci. Technol.* **2016**, *5*, Q35−Q60.

(6) Polyakov, A. Y.; Pearton, S. J.; Frenzer, P.; Ren, F.; Liu, L.; Kim, J. Radiation effects in GaN materials and devices. *J. Mater. Chem. C* **2013**, *1*, 877−887.

(7) Grant, J.; Cunningham, W.; Blue, A.; O'Shea, V.; Vaitkus, J.; Gaubas, E.; Rahman, M. Wide bandgap semiconductor detectors for harsh radiation environments. *Nucl. Instrum. Methods Phys. Res., Sect. A* **2005**, *546*, 213−217.

(8) Yang, G.; Jung, Y.; Kim, B.-J.; Kim, J. Electrical and Optical Damage to GaN-Based Light-Emitting Diodes by 20-MeV Proton Irradiation. *Sci. Adv. Mater.* **2016**, *8*, 160−163.

(9) Ko, G.; Kim, H.-Y.; Bang, J.; Kim, J. Electrical characterizations of Neutron-irradiated SiC Schottky diodes. *Korean J. Chem. Eng.* **2009**, *26*, 285−287.

(10) Fujita, S. Wide-bandgap semiconductor materials: For their full bloom. *Jpn. J. Appl. Phys.* **2015**, *54*, No. 030101.

(11) Ionascut-Nedelcescu, A.; Carlone, C.; Houdayer, A.; von Bardeleben, H. J.; Cantin, J.-L.; Raymond, S. Radiation hardness of gallium nitride. *IEEE Trans. Nucl. Sci.* **2002**, *49*, 2733−2738.

(12) Monroy, E.; Omnès, F.; Calle, F. Wide-bandgap semiconductor ultraviolet photodetectors. *Semicond. Sci. Technol.* **2003**, *18*, R33.

(13) Seo, Y. H.; Nahm, K. S.; Suh, E. K.; Lee, H. J. Growth mechanism of 3C-SiC(lll) on Si without carbonization process. *Korean J. Chem. Eng.* **1996**, *13*, 522−529.

(14) Mastro, M. A.; Kuramata, A.; Calkins, J.; Kim, J.; Ren, F.; Pearton, S. J. Perspective—Opportunities and Future Directions for Ga_2O_3. *ECS J. Solid State Sci. Technol.* **2017**, *6*, P356−P359.

(15) Sasaki, K.; Higashiwaki, M.; Kuramata, A.; Masui, T.; Yamakoshi, S. MBE grown Ga_2O_3 and its power device applications. *J. Cryst. Growth* **2013**, *378*, 591−595.

(16) Oshima, T.; Okuno, T.; Arai, N.; Suzuki, N.; Hino, H.; Fujita, S. Flame Detection by a β-Ga_2O_3-Based Sensor. *Jpn. J. Appl. Phys.* **2009**, *48*, No. 011605.

(17) Oh, S.; Yang, G.; Kim, J. Electrical Characteristics of Vertical Ni/β-Ga_2O_3 Schottky Barrier Diodes at High Temperatures. *ECS J. Solid State Sci. Technol.* **2017**, *6*, Q3022−Q3025.

(18) Higashiwaki, M.; Sasaki, K.; Kuramata, A.; Masui, T.; Yamakoshi, S. Gallium oxide (Ga_2O_3) metal-semiconductor field-effect transistors on single-crystal β-Ga_2O_3 (010) substrates. *Appl. Phys. Lett.* **2012**, *100*, No. 013504.

(19) Hwang, W. S.; Verma, A.; Peelaers, H.; Protasenko, V.; Rouvimov, S.; Xing, H.; Seabaugh, A.; Haensch, W.; Van de Walle, C.; Galazka, Z.; Albrecht, M.; Fornari, R.; Jena, D. High-voltage field effect transistors with wide-bandgap β-Ga_2O_3 nanomembranes. *Appl. Phys. Lett.* **2014**, *104*, No. 203111.

(20) Zhou, H.; Si, M.; Alghamdi, S.; Qiu, G.; Yang, L.; Ye, P. D. High-Performance Depletion/Enhancement-mode β-Ga_2O_3 on Insulator (GOOI) Field-Effect Transistors With Record Drain Currents of 600/450 mA/mm. *IEEE Electron Device Lett.* **2017**, *38*, 103−106.

(21) Oh, S.; Mastro, M. A.; Tadjer, M. J.; Kim, J. Solar-Blind Metal-Semiconductor-Metal Photodetectors Based on an Exfoliated β-Ga_2O_3 Micro-Flake. *ECS J. Solid State Sci. Technol.* **2017**, *6*, Q79−Q83.

(22) Kim, J.; Oh, S.; Mastro, M. A.; Kim, J. Exfoliated β-Ga_2O_3 nanobelt field-effect transistors for air-stable high power and high temperature electronics. *Phys. Chem. Chem. Phys.* **2016**, *18*, 15760−15764.

(23) Blanco, M. A.; Sahariah, M. B.; Jiang, H.; Costales, A.; Pandey, R. Energetics and migration of point defects in Ga_2O_3. *Phys. Rev. B* **2005**, *72*, No. 184103.

(24) Miceli, G.; Pasquarello, A. Energetics of native point defects in GaN: A density-functional study. *Microelectron. Eng.* **2015**, *147*, 51−54.

(25) Gao, F.; Weber, W. J. Empirical potential approach for defect properties in 3C-SiC. *Nucl. Instrum. Methods Phys. Res., Sect. B* **2002**, *191*, 504−508.

DOI: 10.1021/acsami.7b13881
ACS Appl. Mater. Interfaces 2017, 9, 40471−40476

(26) Yang, J.; Ren, F.; Pearton, S. J.; Yang, G.; Kim, J.; Kuramata, A. 1.5 MeV electron irradiation damage in β-Ga_2O_3 vertical rectifiers. *J. Vac. Sci. Technol., B: Nanotechnol. Microelectron.: Mater., Process., Meas., Phenom.* **2017**, *35*, No. 031208.
(27) Ahn, S.; Lin, Y.-H.; Ren, F.; Oh, S.; Jung, Y.; Yang, G.; Kim, J.; Mastro, M. A.; Hite, J. K.; Eddy, C. R., Jr.; Pearton, S. J. Effect of 5 MeV proton irradiation damage on performance of β-Ga_2O_3 photodetectors. *J. Vac. Sci. Technol., B: Nanotechnol. Microelectron.: Mater., Process., Meas., Phenom.* **2016**, *34*, No. 041213.
(28) Ziegler, J. F.; Biersack, J. P.; Ziegler, M. D. *SRIM, the Stopping and Range of Ions in Matter*; SRIM Company, 2008.
(29) Rao, R.; Rao, A. M.; Xu, B.; Dong, J.; Sharma, S.; Sunkara, M. K. Blueshifted Raman scattering and its correlation with the [110] growth direction in gallium oxide nanowires. *J. Appl. Phys.* **2005**, *98*, No. 094312.
(30) Varley, J. B.; Weber, J. R.; Janotti, A.; Van de Walle, C. G. Oxygen vacancies and donor impurities in β-Ga_2O_3. *Appl. Phys. Lett.* **2010**, *97*, No. 142106.
(31) Hajnal, Z.; Miró, J.; Kiss, G.; Réti, F.; Deák, P.; Herndon, R. C.; Kuperberg, J. M. Role of oxygen vacancy defect states in the n-type conduction of β-Ga_2O_3. *J. Appl. Phys.* **1999**, *86*, 3792−3796.
(32) Jun, B.; Subramanian, S. Carrier-removal rate and mobility degradation in heterojunction field-effect transistor structures. *IEEE Trans. Nucl. Sci.* **2002**, *49*, 3222−3229.
(33) Boesch, H. E.; McLean, F. B.; Benedetto, J. M.; McGarrity, J. M.; Bailey, W. E. Saturation of Threshold Voltage Shift in MOSFET's at High Total Dose. *IEEE Trans. Nucl. Sci.* **1986**, *33*, 1191−1197.
(34) Schwank, J. R.; Shaneyfelt, M. R.; Fleetwood, D. M.; Felix, J. A.; Dodd, P. E.; Paillet, P.; Ferlet-Cavrois, V. Radiation Effects in MOS Oxides. *IEEE Trans. Nucl. Sci.* **2008**, *55*, 1833−1853.
(35) Zhang, Z.; Cardwell, D.; Sasikumar, A.; Kyle, E. C. H.; Chen, J.; Zhang, E. X.; Fleetwood, D. M.; Schrimpf, R. D.; Speck, J. S.; Arehart, A. R.; Ringel, S. A. Correlation of proton irradiation induced threshold voltage shifts to deep level traps in AlGaN/GaN heterostructures. *J. Appl. Phys.* **2016**, *119*, No. 165704.
(36) Hu, X.; Karmarkar, A. P.; Jun, B.; Fleetwood, D. M.; Schrimpf, R. D.; Geil, R. D.; Weller, R. A.; White, B. D.; Bataiev, M.; Brillson, L. J.; Mishra, U. K. Proton-irradiation effects on AlGaN/AlN/GaN high electron mobility transistors. *IEEE Trans. Nucl. Sci.* **2003**, *50*, 1791−1796.
(37) Karmarkar, A. P.; Jun, B.; Fleetwood, D. M.; Schrimpf, R. D.; Weller, R. A.; White, B. D.; Brillson, L. J.; Mishra, U. K. Proton irradiation effects on GaN-based high electron-mobility transistors with Si-doped $Al_xGa_{1-x}N$ and thick GaN cap Layers. *IEEE Trans. Nucl. Sci.* **2004**, *51*, 3801−3806.
(38) Ghibaudo, G. New method for the extraction of MOSFET parameters. *Electron. Lett.* **1988**, *24*, 543−545.
(39) Chang, H.-Y.; Zhu, W.; Akinwande, D. On the mobility and contact resistance evaluation for transistors based on MoS_2 or two-dimensional semiconducting atomic crystals. *Appl. Phys. Lett.* **2014**, *104*, No. 113504.
(40) Cao, Q.; Han, S.-J.; Tulevski, G. S.; Franklin, A. D.; Haensch, W. Evaluation of field-effect mobility and contact resistance of transistors that use solution-processed single-walled carbon nanotubes. *ACS Nano* **2012**, *6*, 6471−6477.
(41) Choi, S.-J.; Bennett, P.; Takei, K.; Wang, C.; Lo, C. C.; Javey, A.; Bokor, J. Short-channel transistors constructed with solution-processed carbon nanotubes. *ACS Nano* **2013**, *7*, 798−803.

DOI: 10.1021/acsami.7b13881
ACS Appl. Mater. Interfaces 2017, 9, 40471−40476